Catalysis by Self-Assembled Structures in Emergent Reaction Networks

Gianluca Gazzola[1,2], Andrew Buchanan[1,2],

Norman Packard[1,2], Mark Bedau[1,2,3]*

[1]ProtoLife Srl, Venezia, Italia
[2]European Center for Living Technology, Venezia, Italia
[3]Reed College, Portland, USA
*to whom correspondence should be addressed: mark@protolife.net

Abstract. We introduce a new variant of the dissipative particle dynamics (DPD) model that includes the possibility of dynamically forming and breaking strong bonds. The emergent reaction kinetics may then interact with self-assembly processes. We observe that self-assembled amphiphilic aggregations such as micelles have a catalytic effect on chemical reaction networks, changing both equilibrium concentrations and reaction frequencies. These simulation results are in accordance with experimental results on the so-called "concentration effect."

Keywords: Chemical Reaction Network, Dissipative Particle Dynamics, Self-assembly, Micelle, Concentration Effect.

1 Introduction

We seek to understand the properties of networks of chemical reactions that implicitly interact with self-assembled amphiphilic structures[1]. Chemical reaction networks as well as self-assembled amphiphilic structures[2] are complex systems. Real complex systems in nature often involve the integration of sub-groups of complex systems. The system we study here is one such example. It couples chemical reaction networks with self-assembling amphiphilic structures.

There is ample experimental evidence that such coupled networks exhibit interesting behavior, in particular, that self-assembled amphiphilic structures affect certain chemical reactions. Micelles and other self-assembled structures are known to profoundly increase the rates of certain reactions [11]. The core mechanism is simply that

[1] This is an extended version of a paper with the same title to appear in: Advances in Artificial Life, 9th European Conference ECAL 2007. *Lecture notes in Artificial Intelligence* **2801**, Berlin, Springer (2007).

[2] Various parameters such as temperature, pH, and critical threshold concentration influence the type (or "phase") of structures that self-assemble from the amphiphiles. In addition to familiar amphiphiles such as fatty acids and phospholipids, other materials self-assemble including biopolymers like oligopeptides [12].

the supramolecular structures increase the local concentration of the reagents, just as some catalysts do, and thus accelerate reaction rates. For example, hydrophobic reagents will spontaneously concentrate inside micelles, leading to reaction rate acceleration. Sometimes called "micellar catalysis" [24, 27], this catalytic concentration effect has been observed in a variety of chemical systems that involve micelles and reverse micelles [28, 35]. For example, the presence of micelles increases the rate of RNA self-cleavage reactions 100-fold [27]. Many kinds of reactions are catalyzed by micelles, such as redox [21] and hydrolysis reactions [7]. Micellar catalysis is very general and happens with many kinds of self-assembling materials besides amphiphiles. Examples include polymerized and polymeric amphiphiles [24] and dendrimers [7, 23]. Dendrimers are spherical macromolecules that are somewhat similar to micelles, except that while micelles are rather fluid aggregations composed of many amphiphilic molecules held together by the hydrophobic effect, dendrimers are single static structures tightly held together by covalent bonds.

Our goal here is to model and study this kind of catalysis by self-assembled structures in emergent reaction networks, where the dynamics of the network are not explicitly specified in the rules governing the system. Historically, biochemical reaction networks have been modeled using several approaches. Early approaches used networks whose nodes represented chemical species, and lines between nodes represented reactions. Autocatalytic reaction networks also included lines from catalyst nodes to reaction lines, to represent catalyzed reactions [8, 16]. Other reaction networks have been modeled in immunology: idiotypic networks [9] and more recently, cytokine networks [18]. The chemistry in many of the early network models was abstract. The models intentionally sought to escape from the details of real chemical interactions, for two reasons: capturing the details of real chemical interactions is difficult and immediately begs the question of what level of detail is to be captured, and the results sought from the model were expected (hoped) to be relatively independent from details of the individual chemical reactions; for large networks, the bulk properties of the network (connectivity, scaling, etc.) were hoped to be independent of the details.

More recently, the experimental understanding of reaction networks has been increasing substantially, and there has been an increased awareness of the need to model details of real chemical reactions in order to define and understand biochemical functionality in a given context, e.g., for a cell [29] and for reaction networks with reaction properties based on quantum mechanics [2, 3, 4]. Simultaneously, there has been a growing awareness that chemical reactions cannot by themselves provide a complete picture of biochemical functionality. Structural properties of amphiphilic assemblies must be added to the purely chemical picture. A very rich example is that of lipid structures. These structures are particularly interesting because they have complex phase diagrams, with phase transitions between several different phases, e.g., lipid solution, micelles, and vesicles, because the transitions between these phases may be catalyzed by the presence of other biopolymers, and because some of the phases may themselves have catalytic properties, e.g., for template-directed replication [19, 20, 26]. Finely tuned chemical control of phase transitions in biochemical gels (including more complex gels than simple lipid structures) has been proposed as a general framework for cellular function [25].

In this paper we introduce a model of interacting microscopic particles that combines relatively simple chemical reaction properties with properties deriving from self-assembly processes that can strongly affect the chemical reactions. Interactions between the particles determine both the chemistry and the self-assembly. The macroscopic result of a model simulation is the emergence of a network of chemical reactions that may interact with the self-assembled structures.

2 The model

Our model of chemical reaction systems is based on the well-studied dissipative particle dynamics (DPD) framework [13, 14, 22, 30, 31, 32]. The DPD framework is a mesoscopic system simulator meant to bridge the gap between molecular dynamics (MD) models and continuous substance models. The extreme computational demands of MD models make them appropriate only for simulating small systems for brief intervals—orders of magnitude smaller than the time and length scales of interest here. Continuous substance models are inappropriate as models of molecular scale systems in which the discrete nature of particles impacts the dynamics of the system. In DPD, the equations of motion are second order, with explicit conservation of momentum, in contrast to Langevin or Brownian dynamics. Solvent molecules may be represented explicitly, but random and dissipative forces are included in the dynamics to compensate for the dynamical effects of replacing the hard short-range potentials of MD by softer potentials in DPD simulations. This procedure allows a major acceleration of the simulation compared with MD.

Our work is based on a DPD implementation of a model of monomers and polymers in water. Some elements in the model represent bulk water (one model element representing many molecules). Other elements could represent hydrophilic or hydrophobic monomers. In some cases those elements are connected by explicit bonds, which are represented as springs that freely rotate about their ends. These complexes explicitly but very abstractly represent the three-dimensional structure of polymers. For example, amphiphilic molecules can be created by explicitly bonding a hydrophilic monomer "head" onto a hydrophobic "tail" (chain of hydrophobic monomers).

All the elements move in a two- or three-dimensional continuous space, according to the influences of four forces:

$$f_i = \sum_j \left(F_{ij}^C + F_{ij}^D + F_{ij}^B + F_{ij}^R \right)$$

A weak, conservative force F_{ij}^C governs symmetric pairwise repulsion and attraction of elements. A dissipative force F_{ij}^D causes the kinetic energy of elements to move towards equilibrium with other elements in the region. A random force F_{ij}^R imparts kinetic energy to the elements in arbitrary directions. The strength of the random force is calibrated to balance the lessening of system energy due to the dissipative force, maintaining the temperature at a fixed average value, with fluctuations about this average depending on the system size. All of these forces are considered to oper-

ate only within a certain local cutoff radius r_0. The cutoff radius is a primary mechanism for improving model computational efficiency. In all the simulations presented here, the cutoff radius has unit length, $r_0 = 1$. Elements that are strongly bonded to other elements are also influenced by the movement of those elements to which they are bonded, through F_{ij}^{B}, the spring force that connects them.

We will now further specify DPD's two distinct types of particle interaction. The first type of particle interaction is referred to as "strong bonds," which represent covalent chemical bonds. All strong bonds in DPD are specified initially, and subsequently cannot form or break. Strong bonds are modeled by a Hookian law spring:

$$F_{ij}^{B} = k\left(r_{ij} - l\right),$$

where r_{ij} is the Euclidean distance between the particles, k is the spring constant specifying the strength of the bond, which in our simulations has the same value for all strong bonds, and l is the relaxed bond length. The spring constant is set to $k = 100$ and the spring distance is set to $l = 0.01$ for our simulations. For simplicity, the DPD chemical bonds discussed here have the restriction that each element can have at most two strong bonds at a given time, allowing the formation of polymers, but not more complex chemical structures.

The second type of particle interaction are weak, conservative forces, which represent associations resulting from Van der Waals forces or hydrogen bonds, for example. Weak interactions are typically modeled by the Lennard-Jones potential:

$$U(r_{IJ}) = \alpha_{IJ}\left(\frac{1}{r_{IJ}^{12}} - \frac{\beta_{IJ}}{r_{IJ}^{6}}\right),$$

with α_{IJ} and β_{IJ} and specific to the types of I and J, or by various linear approximations. In the work presented here, we use a linear function for the conservative force, following [5]:

$$F_{ij}^{C} = \alpha_{IJ}\left(1 - \beta_{IJ}\, r_{ij}\right)$$

Different parameter values are possible for interactions between different particle types. Orientation of individual elements also plays no role, as the forces affecting DPD elements are radially symmetric. The pairing that occurs is a cooperative phenomenon, as are structures that self-assemble as a result of these forces.

The dissipative force is calculated by:

$$F_{ij}^{D} = \gamma\left(v_i - v_j\right)\left(1 - r_{ij}\right)^2,$$

where v_i is the velocity of *i*, γ is a weighting factor given by $\gamma = \sigma^2/2$ and σ is a balancing factor between dissipative and random forces which serves to maintain the temperature of the system around a more or less fixed point.

The random force is calculated by

$$F_{ij}^{R} = \sigma w^{R}\left(1-r_{ij}\right)u,$$

where w^R is an independent random factor and *u* is a uniform random number chosen from the interval (-1,1). In our simulations, σ=3 and w^R=2.73205 (calibrated to give appropriate random fluctuations for water particles).

A DPD system with the forces listed above can create self-assembled structures held together with the weak associative forces. For example, a DPD system with amphiphiles in water can exhibit a wide variety of the known amphiphilic phases, including monolayers, bilayers, micelles, rods, vesicles, and bicontinuous cubic structures [17, 15, 30, 33, 34].

We augmented the standard DPD framework [1, 6] to introduce the possibility of chemical reactions by making strong bonds dynamic. This dynamic-bonding DPD (or dbDPD) adds a new characteristic of reactivity for particles, with the following two rules for reactive particles:

1. Bonds form between reactive particles *i* and *j* if elements come within the bond-forming radius, $r_{ij} < r_{IJ}^{f}$, ($r_{IJ}^{f} = 0.2$ in our simulations).
2. Bonds break between reactive particles *i* and *j* if bonded elements go outside the bond-breaking radius, $r_{ij} > r_{IJ}^{b}$, ($r_{IJ}^{b} = 0.4$ in our simulations).

Not all particles need be reactive; only reactive particles are affected by these new rules. The strong bond strength parameter *k* governs the strength of all strong bonds, whether or not they were present in the initial conditions.

For the present simulations, we make no attempt to enforce strict energy conservation during the bond formation and breaking processes, and so small amounts of energy are added to the system when bonds are formed, and taken from the system when bonds are broken. However, the momentum in the system is constant, since the changes in the momentum of individual elements due to bonding events is always symmetrical with respect to the bonded particles. Note also that after an initial transient, bond formation events equilibrate with bond breaking events, so the temperature stabilizes.

3 Emergent Chemical Reaction Networks

Some of the networks in the literature are emergent [2, 16], some not. Reaction networks that arise as a result of our chemistry within dbDPD are highly emergent, in the sense that their equilibrium state is very hard to derive without explicit simulation.
Given rules for forming and breaking bonds, together with the constraint of only two or less bonds allowed per particle, we have the basis for a network of polymerization reactions. The architecture of the reaction network is determined by the constraints that are set on the process of strong bond formation. The reaction network complexity is controlled with the specification of the pairs of particle types that can form strong bonds and of the maximum length *N* of the polymeric chains resulting from the strong bond formation process.

The simple example we explore first is a reaction network identified by the duple <{5,4}, 2>, namely having two reactive particle types labeled with integers 5 and 4 that can only form chains of length *N*=2, resulting in the architecture shown in Fig. 1.

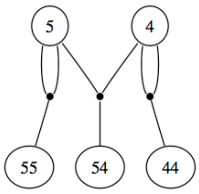

Fig. 1. Architecture of the reaction network for the first experiment, polymerization from monomers to dimers.

Each labeled node represents a chemical species that can undergo strong bonding reactions; each solid dot connecting edges from the chemical species represents one of the three possible reactions that can take place:

$$5 + 4 \longleftrightarrow 54$$
$$5 + 5 \longleftrightarrow 55$$
$$4 + 4 \longleftrightarrow 44$$

Note that bond forming and bond breaking radii don't influence a chemical reaction network's architecture, but play a main role in determining the rate of interaction of reagents in the process of strong bond formation. In our simulations the values of r_{IJ}^{f} and r_{IJ}^{b}, with $r_{IJ}^{f} < r_{IJ}^{b}$, were the same for all reagents. Thus we can say that all reagents share the same intrinsic reaction rate.

3.1 Results in a simple network

The first experiment we report concerns a simple network that contains five particle types: water (type 1), amphiphilic heads (type 2), amphiphilic tails (type 3), and two reagents (types 4 and 5). Because it is so simple, this network clearly illustrates the main kinds of interactions between self-assembled structures and emergent reaction networks.

The inter-particle interactions use the linear function described above, with $(\alpha_{IJ}, \beta_{IJ})$ values specified in Table 1.

Table 1. $(\alpha_{IJ}, \beta_{IJ})$ values for particle interactions in simple network. The particle types 4 and 5 are the monomers that polymerize in the reaction network.

$(\alpha_{IJ}, \beta_{IJ})$	water	head	tail	4	5
water	(1,1)				
head	(1,1)	(150,1)			
tail	(4,1)	(15,5)	(5,1)		
4	(1,1)	(1,5)	(1,1)	(1,1)	
5	(1,1)	(1,5)	(1,1)	(1,1)	(1,1)

Note that "neutral" interactions, e.g. between water and water, are taken to be very weak repulsive interactions, with $(\alpha_{IJ}, \beta_{IJ})$ = (1,1).

The self-assembly process of amphiphilic dimers into micelles can require several time steps in DPD, depending on several factors, such as the temperature of the system and the strength of the weak forces. In our experiments, we wanted to simulate a real chemical system in which lipophilic reagents are placed into an aqueous solution containing micelles that have already formed. In control cases, the amphiphilic dimers were replaced by water and particle initial positions were chosen randomly. All the other DPD parameters were kept the same.

The experiments that we ran were set within a 30x30 toroidal space with 7200 particles, composed of 2/7 reagents, 2/7 amphiphilic dimers and 3/7 water. Simulations were run without allowing the reagents to form bonds, until the amphiphiles aggregated into micelles and the distribution of reagents reached the equilibrium, according to the weak forces that reagents feel towards amphiphiles. Then the particle positions were saved and the simulation was restarted loading those positions as initial conditions.

Fig. 2 shows a picture of the DPD simulation for the control case (without the micelle-forming dimers) and the experiment (with micelle forming dimers). Fig. 3 shows a time series of the concentrations of all chemical species present in the reaction network of Fig. 1. Note that the equilibrium concentrations (long-time average concentrations) are radically different for the control vs. the experiment.

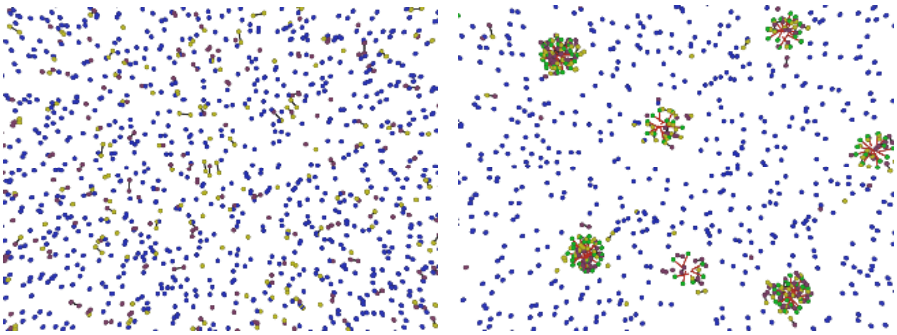

Fig. 2. DPD simulation of the control (left) with no amphiphilic dimers, and the experiment (right) with amphiphilic dimers.

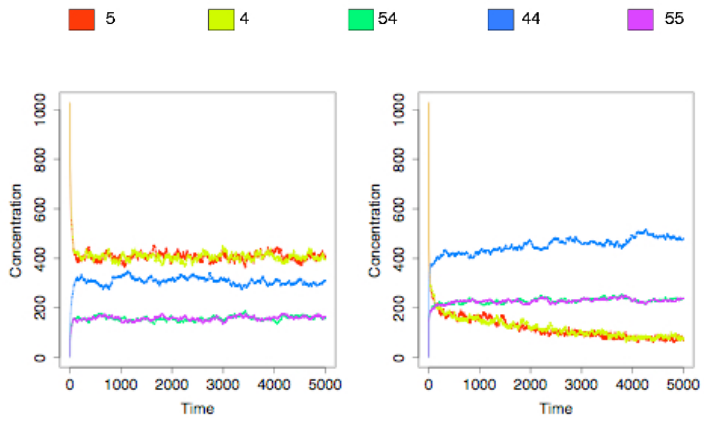

Fig. 3. Concentration time series of different chemical species for control (left) and experiment (right). At long times, the concentrations fluctuate about equilibrium.

One straightforward way to compare the behavior of the system with micelles to a control without micelles is by analyzing the average concentrations of the species identified by the network's nodes at equilibrium. As we can see from Fig. 4 and Table 2, in the control case concentrations fall into three clearly distinguishable classes. The dominant species are monomers, followed by the only non-palindromic dimer and then by the two palindromic dimers, produced by a self-reaction, which is a reaction between two monomers of the same kind. The experimental case is, in contrast, dominated by the non-palindromic dimer, followed by the two non-palindromic ones and then by monomers. Note that palindromic dimers are half as concentrated as non-palindromic dimers in both systems.

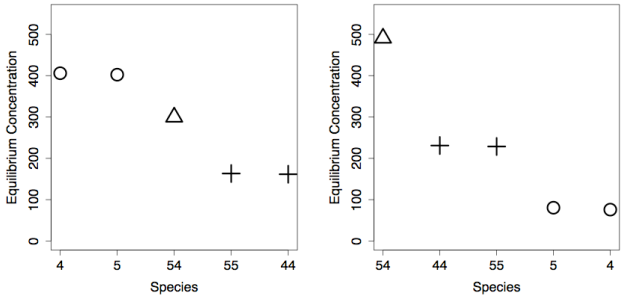

Fig. 4. Equilibrium concentration of different chemical species for a representative dbDPD run of control (left) and experiment (right). The error bars are smaller than the size of the symbols. Note that the triangle has the highest concentration for the experiment, shifted significantly from the control.

Table 2. Equilibrium concentration for each chemical species as shown in Fig. 4.

Chemical species	Equilibrium concentration	Length
CONTROL		
4, 5	~ 404	Monomers
54	~ 300	Non-palindromic dimer
44, 55	~ 162	Palindromic dimers
	EXPERIMENTAL	
54	~ 491	Non-palindromic dimer
44, 55	~ 230	Palindromic dimers
5, 4	~ 79	Monomers

Table 3. Reaction frequency for the same run as in Figs. 2-4 and Table 2.

Chemical reactions	Reaction frequency	Observations
CONTROL		
5 + 4 ↔ 54	~ 103	Monomer + monomer ↔ non-palindromic dimer
5 + 5 ↔ 55 4 + 4 ↔44	~ 52	Monomer + monomer ↔ palindromic dimer
EXPERIMENTAL		
5 + 4 ↔ 54	~ 88	Monomer + monomer ↔ non-palindromic dimer
5 + 5 ↔ 55 4 + 4 ↔44	~ 42	Monomer + monomer ↔ palindromic dimer

We may also compare the reaction dynamics of the two systems, in particular, how frequently reactions happen. Table 3 displays how often each possible reaction happens on average over 50 time steps once the dynamics have reached the equilibrium. In both the control and the experimental case reaction frequencies fall into two classes, the one containing the self-reactions and the other one the non–self-reactions. Note that in both cases, the reactions that involve palindromic dimers are half as frequent as those that involve non-palindromic ones. The experimental case shows that the frequency of each reaction is lower than its corresponding one in the control. We now discuss two different observed effects in detail.

Concentration effect: In the control case the only force that can keep the reagents close to each other is due to the (possible) strong covalent bonds formed between two of them. As we said above, if two reagents come within a distance smaller than their bond forming radius, then they form a strong bond that keeps on existing as long as the reagents' distance is smaller than their bond breaking radius. The reagents are free to float around until they form a strong bond. At this point, the bond strength will determine how long the bonded monomers will stay close to each other enough to keep their bond intact. The weaker the bond, the more likely it will be for it to get broken in the following time steps, leaving the two resulting monomers free floating again. Apart from the bond strength, nothing affects the survival probability of a dimer.

In the experimental case, clusters of reagents form because of the weak forces that attract them to micelles. Therefore when the covalent bonds are broken, the monomers don't start to freely diffuse again, but continue to be entrapped in the same cluster, then it is very likely that they are involved in new bonding reactions, possibly with other free monomers in the same cluster

The probability of existence of a bond depends on several factors. One main factor is the reagents' density (number of reagents over space area). The higher the density, the smaller the average distance between reagents. This probability affects equilibrium concentrations. If bonds are highly likely, then longer polymers are more prevalent. If bonds are unlikely, then monomers are more prevalent. For the reasons we explained above, the reagent density is locally increased by micelles, and that explains why dimers are more concentrated than monomers. By spatially concentrating reagents the micelles act as catalysts. We could also have obtained an analogous result in the control case, by increasing the bond strength.

The concentration effect caused by micelles can be observed from the change in reaction frequencies. Due to the concentration effect, bonded dimers survive for a longer time than when there is no concentration effect, reducing the frequency of the bond breaking reactions. This results in a low number of free reactive monomers, which decreases the frequency of the forward reactions as well.

Palindrome effect. We noticed that the 55 and 44 dimers' concentration is around half of that of the 54 dimer at equilibrium (Fig. 4, Table 2). We also noticed that the frequency of each reaction involving 55's or 44's is half as much of that of the only reaction that involves 54's. The reason is that dimers 54 and 45 have been identified as the same dimer. For all possible pairwise combinations of monomers of type 4 and type 5, if 4's are as many as 5's, there are equal numbers of 44, 45, 54, and 55, so if 45 and 54 are considered identical, their number is double that of 44 and 55. More generally, one may consider all polymer types of a given length, and see by the same

argument that those that are non-palindromic will be doubled by identifying polymers read in one direction with those that are the same when read in the opposite direction.

While the concentration effect concerns the difference between control and experimental equilibria, the palindrome effect concerns the difference between palindromic and non-palindromic *N*-mers in either control or experimental situations. The palindrome effect is actually seen in both the control and the experimental case.

3.2 Results for a larger network

We observed qualitatively the same kinds of effects in a wide variety of more complex emergent reaction networks, with higher maximum polymer length and more kinds of reagents. The goal was to understand if and how the behaviors observed in the simple network described above, could be qualitatively confirmed. We briefly present here the results from the network <{6,5,4}, 3>, made up of 27 nodes and 33 branches (Fig. 5), versus 5 and 3 respectively in the simple example.

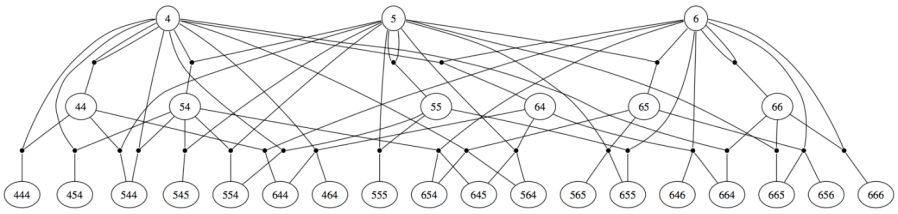

Fig. 5. Architecture of the more complex reaction network, polymerization of dimers and trimers from three species of monomers.

The $(\alpha_{IJ}, \beta_{IJ})$ values specifying inter-particle interactions in the network in Fig. 5 are the same as those for the simpler network, with particle type 6 matching particles 4 and 5.

Fig. 6 shows a time series of the concentrations of representative chemical species present in the reaction network of Fig. 5. Note that the equilibrium concentrations are radically different for the control vs. the experiment (Fig. 7). In particular, when we compare the experimental equilibria with the control case, the increased concentration of the trimers (both palindromic and non-palindromic) and the decreased concentration of the monomers is an instance of the concentration effect. Just as in the simpler network, the self-assembled micelles act as catalysts by concentrating reagents. Fig. 7 also illustrates the palindrome effect, as expected, for in both the control and experimental cases, non-palindromic N-mers have double the concentration of palindromic N-mers.

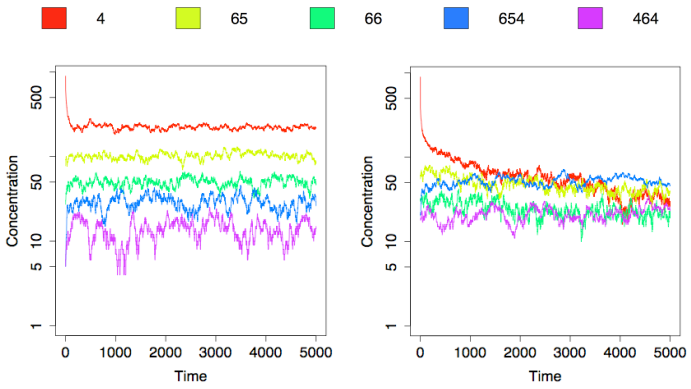

Fig. 6. Time series of concentration of representative chemical species for control (left) and experiment (right). The log scale on the y-axis helps resolve low concentration species. At long times, the concentrations fluctuate about equilibrium.

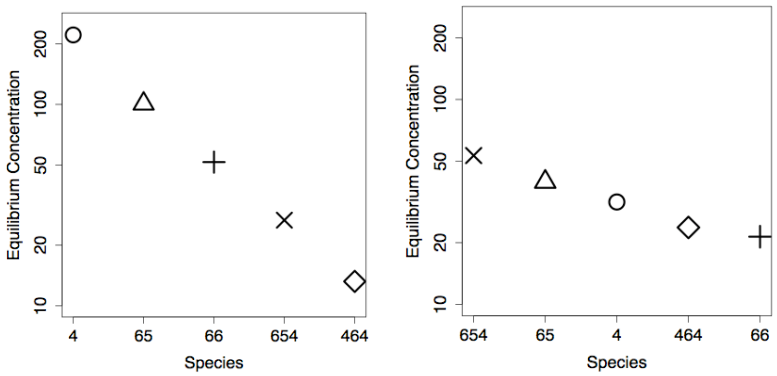

Fig. 7. Equilibrium concentrations of representative chemical species for control (left) and experiment (right). The error bars are smaller than the size of the symbols. The log scale on the y-axis is to aid comparison with Fig. 6. Note that the trimers concentrations are significantly higher in the experiment.

Cascade effect: The more complex networks illustrated a third effect. Micelles increase the frequency of the reactions involving higher length polymers, as they tend to increase the concentration of their required ingredients compared to the control case. On the way to equilibrium, however, we see that first monomer concentration decreases as dimer concentration rises, then, after reaching a maximum, dimer concentration decreases as trimer concentration increases, and so on. We term this effect moving through successive length polymers the “cascade effect”.

4 Discussion and Conclusion

We have studied a new variant of dissipative particle dynamics (DPD) with dynamic bond forming and breaking, which we termed "dbDPD". This yields a microscopic mechanism for chemical reactions, from which emerges macroscopic chemical kinetics. The reagents may be represented as nodes on a graph, the reaction network, which also emerges from the microscopic chemical reaction mechanism. The emergent reaction network and reaction kinetics have many of the hallmarks of real reaction networks, e.g., the existence of many side reactions Here, we have studied a particular class of reactions, polymerization between two or three monomer types.

DPD is well known as a modeling framework that is suited for studying self-assembled structures from amphiphilic molecules. Our addition of chemical reactions in dbDPD enables the additional study of the interplay between chemical reactions and self-assembly processes.

We report a clear identification of an experimentally known type of micellar catalysis: the concentration effect. Essentially, the effect comes about because lipophilic reagents may aggregate within or near the micelles, effectively increasing their local concentration and changing the equilibrium concentrations of resulting reaction products. In particular, long polymers that have very low equilibrium concentration in the absence of micelles may have very high equilibrium concentration (relative to all other reagents) in the presence of micelles.

In addition to the concentration effect, we identified two other effects that should be experimentally observable: (i) the palindrome effect, the doubling of the concentration of non-palindromic polymers because of the identification of polymers read in one directions with those that are the same when read in the opposite direction, and (ii) the cascade effect, seen when starting with high concentration of monomers: the concentration of monomers goes down as the concentration of dimers increases, then the concentration of dimers reaches a maximum and then decreases as the concentration of trimers increases, and so on.

Future directions for research based on dbDPD include refinement of the microscopic chemical reaction mechanisms to make them more realistic for particular target experiments. We also believe that introduction of variations into reaction products may enable the system to display evolvability.

Acknowledgements. We thank JohnMcCaskill and Thomas Maeke for an implementation of DPD software from which our software is derived. We benefited from conversations with Harold Fellermann, Ricard Solé, and Martin Hanczyc. Thanks also to the ECLT, which helped facilitate this work and provided an opportunity to present it. This work was supported by the EU in the PACE integrated project, EC-FP6-IST-FET-IP-002035.

References

1. Bedau M. A., Buchanan A., Gazzola G., Hanczyc M., Maeke T., McCaskill J. S., Poli I. and Packard N. H., Evolutionary design of a DDPD model of ligation. *Lecture Notes in Computer Science* **3871**, (2005) 201-212.
2. Benkö G., Flamm C. and Stadler P.F., A Graph-Based Toy Model of Chemistry. Journal of Chemical Information and Computational Science **43** (2003) 1085-1093.
3. Benkö G., Flamm C. and Stadler P.F., Generic Properties of Chemical Networks: Artificial Chemistry Based on Graph Rewriting, in Banzhaf W., Christaller T., Dittrich P., Kim J. T., and Ziegler J. (Eds.), Advances in Artificial Life: Proceedings of the 7th European Conference on Artificial Life (ECAL), Springer Verlag, Berlin (2003) 10-19.
4. Benkö G., Flamm C. and Stadler P.F., Multi-Phase Artificial Chemistry, in H Schaub, F. Detje, U. Brüggemann (Eds.), The Logic of Artificial Life: Abstracting and Synthesizing the Principles of Living Systems, IOS Press, Akademische Verlagsgesellschaft, Berlin (2004), 16-22.
5. Besold G., Vattulaien I., Karttunen M., Polson J. M., Towards Better Integrators for Dissipative Partycle Dynamics Simulations. *Physical Review E* **62** (2000) 7611-7614.
6. Buchanan A., Gazzola G., Bedau M. A., Evolutionary Design of a Model of Self-Assembling Chemical Structures, in Natalio Krasnogor, Steve Gustafson, David Pelta and Jose L. Verdegay (Eds.), Elsevier Science, Amsterdam (2007).
7. Delort E., Darbre T. and Reymond J.-L., A Strong Positive Dendritic Effect in a Peptide Dendrimer-Catalyzed Ester Hydrolysis Reaction. *Journal of the American Chemical Society **126*** (2004) 15642-15643.
8. Farmer J.D., Kauffman S.A. and Packard, N.H.: Autocatalytic Replication of Polymers. *Physica D* **22** (1986) 50.
9. Farmer, J.D., Packard N.H. and Perelson A.: The Immune System, Adaptation, and Machine Learning, *Physica D* **22** (1986) 187.
10. Fellerman, H., Rasmussen, S., Ziock, H., Solé, R. (2007). Life cycle of a minimal procell: a dissipative particle (DPD) study. *Artificial Life*, in press.
11. Fendler J. H. and Fendler E. J., *Catalysis in micellar and macromolecular systems*. Academic Press, New York (1975).
12. Fung S. Y., Keyes C., Duhamel J. and Chen P.: Concentration Effect on the Aggregation of a Self-Assembling Oligopeptide. *Biophysical Journal* **85** (2003) 537–548
13. Groot R. and Warren P., Dissipative particle dynamics: bridging the gap between atomistic and mesoscopic simulations. *Journal of Chemical Physics* **107** (1997) 4423–4435.
14. Hoogerbrugge P. and Koelman J.: Simulating microscopic hydrodynamic phenomena with dissipative particle dynamics. *Europhysics Letters* **19** (1992) 155–160.
15. Jury S., Bladon P., Cates M., Krishna S., Hagen M., Ruddock N. and Warren P.: Simulation of amphiphilic mesophases using dissipative particle dynamics. *Physical Chemistry and Chemical Physics* **1** (1999) 2051–2056.
16. Kauffman S. A., Autocatalytic sets of proteins. *Journal of Theoretical Biology*, **119** (1986) 1-24.

17. Kranenburg M., Venturoli M. and Smit B., Phase behavior and induced interdigitation in bilayers studied with dissipative particle dynamics. *Journal of Physical Chemistry* **107** (2003) 11491–11501.
18. Kuby J.: *Immunology*, 3rd ed.,W. H. Freeman, New York (1997).
19. Luisi P.L., Giomini M., Pileni M., and Robinson B., Reverse micelles as hosts for proteins and small molecules. *Biochimica and Biophysica Acta* **947** (1988) 209-246.
20. Luisi P.L., Walde P. and Oberholzer T., Enzymatic synthesis in self-reproducing vesicles: An approach to the construction of a minimal cell. *Berichte der Bunsengesellschaft für Physikalische Chemie* **98** (1994) 1160-1165.
21. Mallick K., Jewrajka S., Pradhan N. and Pal T., Micelle-catalysed redox reaction. *Current Science* **80** (2001) 1408-1412
22. Marsh, C.: Theoretical aspects of dissipative particle dynamics. University of Oxford, Ph.D. Thesis (1998).
23. Martin K. I. and Twyman L. J., Acceleration of an aminolysis reaction using a PAMAM dendrimer with 64 terminal amine groups. *Tetrahedron Letters* **42** (2001) 1123–1126.
24. Oehme G., Grassert I., Paetzold E., Fuhrmann H., Dwars T., Schmidt U. and Iovel I., The Effect of Assembled Amphiphiles on Catalytic Reactions in Aqueous Media. *Kinetics and Catalysis,* **44** (2003) 766–777.
25. Pollack G. H., *Cells, Gels and the Engines of Life: A New, Unifying Approach to Cell Function*, Ebner & Sons, Seattle, WA, USA (2001).
26. Rasmussen S., Chen L., Stadler B. and Stadler P., Proto-organism kinetics: Evolutionary dynamics of lipid aggregates with genes and metabolism, *Origins of life and evolution of the biosphere* (in press).
27. Riepe A., Beier H. and Gross H. J., Enhancement of RNA self-cleavage by micellar catalysis. *FEBS Letters* **457** (1999) 193-199.
28. Ruasse M.-F., Blagoevab I. B., Garcia-Rio R. C. L. G., Leis J. R., Marques A., Mejuto J. and Monnier E., Organic reactions in micro-organized media: Why and how? *Pure and Applied Chemistry,* **69** (1997) 1923-1932.
29. Shilling C. H. and Palsson B. O., The underlying pathway structure of biochemical reaction networks, *Proceedings of the National Academy of Science* **95** (1998) 4193–4198.
30. Shillcock J. and Lipowsky R., Equilibrium structure and lateral stress distribution from dissipative particle dynamics simulations. *Journal of Chemical Physics* **117** (2002) 5048–5061.
31. Trofimov S., Nies E. and Michels M., Thermodynamic consistency in dissipative particle dynamics simulations of strongly nonideal liquids and liquid mixtures. *Journal of Chemical Physics* **117** (2002) 9383–9394.
32. Vattulainen I., Karttunen M., Besold G. and Polson J.: Integration schemes for dissipative particle dynamics simulations: From softly interacting systems towards hybrid models. *Journal of Chemical Physics* **116** (2002) 3967–3979.
33. Yamamoto S., Maruyama Y. and Hyodo S.: Dissipative particle dynamics study of spontaneous vesicle formation of amphiphilic molecules. *Journal of Chemical Physics* **116** (2002) 5842–5849.
34. Yamamoto S., Hyodo, S.: Budding and fission dynamics of two-component vesicles. *Journal of Chemical Physics* **118** (2003) 7937–7943.
35. Zingaretti L., Boscatto L., Chiacchiera S. M. and Silber J. J. **:** Kinetics and mechanism for the reaction of 1-chloro-2,4-dinitrobenzene with n-butylamine and piperidine in AOT/n-hexane/water reverse micelles. *Arkivoc* **X** (2003) 189-200.